Bull. Mater. Sci., Vol. 38, No. 2, April 2015, pp. 493–498. © Indian Academy of Sciences.

Room temperature synthesis of crystalline Sb_2S_3 for SnO_2 photoanode-based solar cell application

ANIL N KULKARNI[1,3,*], SANDEEP A AROTE[2], HABIB M PATHAN[2] and RAJENDRA S PATIL[1]

[1]Department of Physics, PSGVPM's ASC College, Shahada 425 409, India
[2]Advanced Physics Laboratory, Department of Physics, Savitribai Phule Pune University, Pune 411 007, India
[3]Department of Applied Physics, Cummins College of Engineering, Pune 411 052, India

MS received 3 May 2014

Abstract. **The preparation of crystalline antimony sulphide (Sb_2S_3) by chemical route at room temperature was reported in this paper. The structural, morphological and optical properties of as-synthesized sample were systematically investigated. X-ray diffraction (XRD) analysis confirms the orthorhombic crystal phase for prepared Sb_2S_3. Scanning electron microscope (SEM) images show uniform, dense spherical morphology having diameter around 200–220 nm. Energy band gap calculated from optical absorption spectra was observed around 2.17 eV. Contact angle measurement confirms the hydrophilic nature of the deposited film. The photoluminescence analysis shows low green luminescence as well as Stoke's shift for as-prepared Sb_2S_3. The nanostructured solar cell is fabricated for energy harvesting purpose with Sb_2S_3-sensitized SnO_2 photoanode and polysulphide electrolyte. The solar cell with FTO/SnO_2/Sb_2S_3 photoanode shows $V_{OC} \sim 240$ mV, $J_{sc} \sim 0.640$ mA cm^{-2} and FF $\sim 35\%$. The working mechanism and energy level diagram of Sb_2S_3/SnO_2 system have been discussed.**

Keywords. **Sb_2S_3; crystal phase; photosensitization.**

1. Introduction

In recent times, the ability of nanostructured solar cell with dye sensitized metal oxide as photoanode has received attention of researchers owing to their low cost, simple fabrication technique and feasibility.[1] Although the dye-sensitized solar cells (DSSCs) have considerable conversion efficiency, the complex structure of dyes, their availability and stability put certain constrains on their industrial applications.[2] Therefore, nowadays semiconductor materials with narrow band gap are attractive alternative to the light-harvesting dye molecules because of their tunable electrical, optical and structural properties.[3,4] The semiconductor with unique properties like tunable band gap over a wide range to match the solar spectrum, good photostability, broad excitation spectra, high extinction coefficient and multiple exciton generation capability makes them potentially suitable for photovoltaic's applications.[3] Some previous investigations in this concern have been carried out using CdS,[4–6] CdSe,[7–10] Ag_2S,[11] In_2S_3,[12] PbS,[13] Sb_2S_3[14] semiconductor nanoparticles. Among these Sb_2S_3 has attracted attention of the researchers owing to its narrow band gap of about 1.7 eV which can allow extension of the absorption band toward the near infrared (NIR) part of the solar spectrum.[14] Sensitization with Sb_2S_3 nanoparticles also helps in multiple exciton generation and enhancement in the charge separation process.[15] Many reports are available on the deposition of Sb_2S_3 thin films by chemical route,[16–18] while synthesis of crystalline Sb_2S_3 at room temperature is seldom reported.[19] Although Sb_2S_3 has more compatible properties for photovoltaic applications, very few reports are available on TiO_2/Sb_2S_3 configuration.[20–22] However, so far SnO_2/Sb_2S_3 system has not been studied for energy harvesting purpose.

With this inspiration, in the present study, we report for the first time, the preparation of crystalline Sb_2S_3 by chemical bath deposition at room temperature. Deposited Sb_2S_3 is used for the fabrication of Sb_2S_3 sensitized SnO_2 photoelectrode *via* the doctor blade method to explore the system for nanostructured solar cell application. The working mechanism and energy level diagram of Sb_2S_3/SnO_2 system have been discussed.

2. Experimental

2.1 *Synthesis of Sb_2S_3, preparation of SnO_2 photoelectrode and fabrication of solar cell*

Chemical bath deposition (CBD) has been followed for the synthesis of nanospheres of Sb_2S_3. Depositions were conducted at room temperature for 1 h using a solution mixture of antimony chloride and sodium thiosulfate ($Na_2S_2O_3$) as a precursor source of Sb^{3+} and S^{2-} ions, respectively.[19] Ethylene diamine tetraacetic acid (EDTA) was used as complexing agent.

To make SnO_2 paste, 0.5 g of SnO_2 powder was mixed with ethanol, acetic acid, ethylene glycol and α-terpineol in

*Author for correspondence (kulkarni.may29@gmail.com)

mortar and pestle for 40 min, then SnO_2 film was prepared on fluorine-doped tin oxide (FTO) glass by the doctor blade method.[23] After drying, all samples were annealed at 450°C for 1 h. Further the SnO_2 films were immersed into Sb_2S_3 colloidal solution for 1 h to adsorb Sb_2S_3 nanoparticles onto the SnO_2 photoelectrode surface.

The solar cell was assembled with Sb_2S_3 sensitized SnO_2 photoanode, polysulphide as electrolyte and carbon coated FTO as a counter electrode. For fabrication of solar cell, few drops of polysulphide electrolyte solution were added between Sb_2S_3/SnO_2 photoelectrode and counter electrode (carbon-coated FTO). Finally, they were clamped together facing conducting surfaces inwards.

The structural analyses were carried out by RigakuDmax-2400 (Cu Kα = 0.154 nm) X-ray diffractometer. The optical absorbance was recorded on JASCO V-670 spectrophotometer and the emission spectrum was recorded by using Perkin Elmex LS55 photoluminescence spectroscopy technique with He–Ne LASER line (325 nm) as excitation source at room temperature. The morphology of the deposited films was studied by JEOL-JSM 6360 scanning electron microscope (SEM). *J–V* measurements were conducted in the dark and under an illumination of 50 mW cm^{-2} to study the performance of fabricated solar cell.

3. Results and discussion

3.1 *Structural analysis*

Phase and purity of prepared Sb_2S_3 nanospheres were confirmed from X-ray diffraction (XRD) analysis as shown in figure 1a. The XRD pattern shows defined peaks around 2θ = 28.85°, 32.13° and 45.75°, indexed to the diffraction from the (321), (221) and (441) planes, respectively. Almost single larger intensity peak with smaller full-width at half-maxima (FWHM) was observed, indicating highly oriented and crystalline nature of the prepared Sb_2S_3 nanospheres. Defined peaks match with the standard peaks from JCPDS file no. 42-1393, readily confirm the orthorhombic phase for Sb_2S_3. Many reports are available on the synthesis of polycrystalline Sb_2S_3 deposited at various bath temperatures (low as well as high).[19,24] The elemental analysis of prepared Sb_2S_3 was carried out by energy-dispersive spectroscopy (EDS). Figure 1b gives the average atomic percentage of Sb:S as 53.46, revealing the typical stochiometric formation of the antimony sulphide at room temperature.

The average crystallite size of the as-prepared Sb_2Se_3 was predicted by the Scherer formula,[25]

$$D = \frac{0.9\lambda}{\beta \cos \theta}, \quad (1)$$

where λ (= 1.54 Å) is the wavelength of the X-rays, β the full-width in radians at half-maximum of diffraction peaks and θ Bragg's angle of the X-ray pattern at maximum intensity. The average crystallite size estimated is in the range of 30–60 nm in crystalline orientations of (321), (221) and (441) planes.

3.2 *Contact angle measurement*

The water contact angle measurement was performed for the films of antimony sulphide, in order to get information about the surface wetting capacity of the deposited material. The water droplet was poured with the help of syringe onto the surface of as-deposited films of Sb_2S_3 and the images of the drop were captured as shown in figure 2. It has been observed that the angle of contact for films of antimony sulphide with water around 50°. The acute angle of contact reveals the hydrophilic nature of the prepared Sb_2S_3 nanospheres.

3.3 *Morphological analysis of Sb_2S_3, SnO_2 and SnO_2/Sb_2S_3 thin films*

The typical SEM images of as-deposited Sb_2S_3 in figure 3a show the well-distributed spherical morphology. The study carried out by Lokhande *et al*[19] also showed the spherical

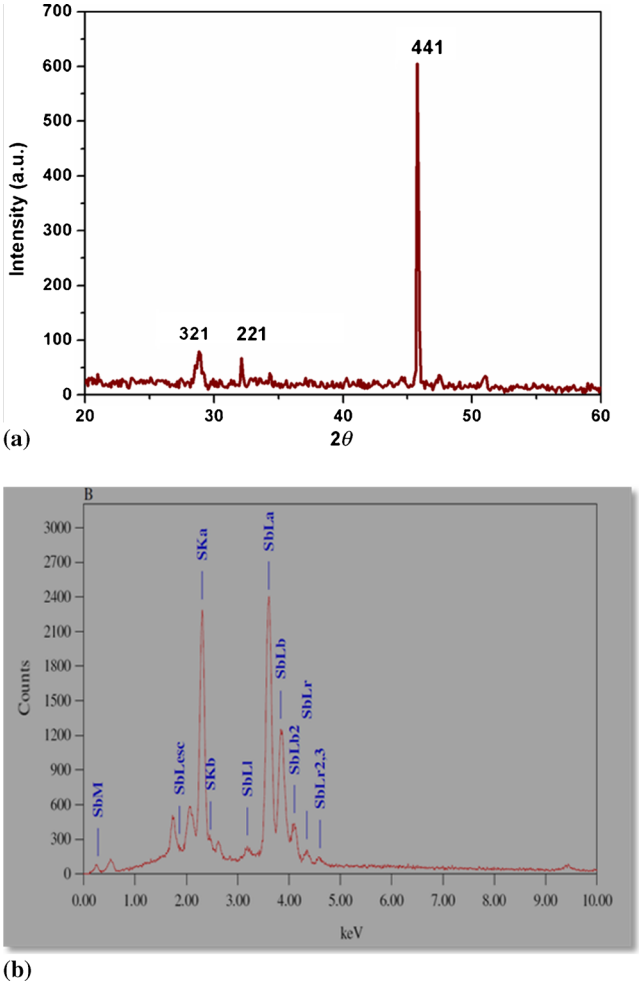

Figure 1. (**a**) XRD pattern of Sb_2S_3 deposited at room temperature and (**b**) EDS spectrum of Sb_2S_3 deposited at room temperature.

morphology for antimony sulphide, deposited at very low temperature (6 ± 2°C). While, Han *et al*[26] observed olivary microcrystallines of Sb_2S_3 synthesized *via* a hydrothermal procedure at high temperature about 180°C. An observation from figure 3b and c reveals that after Sb_2S_3 sensitization, the morphology of SnO_2 photoelectrode changes from porous nanoparticles network to the well-developed flakes like structure. The observed changes in the surface morphology is attributed to the growth of Sb_2S_3 on SnO_2.

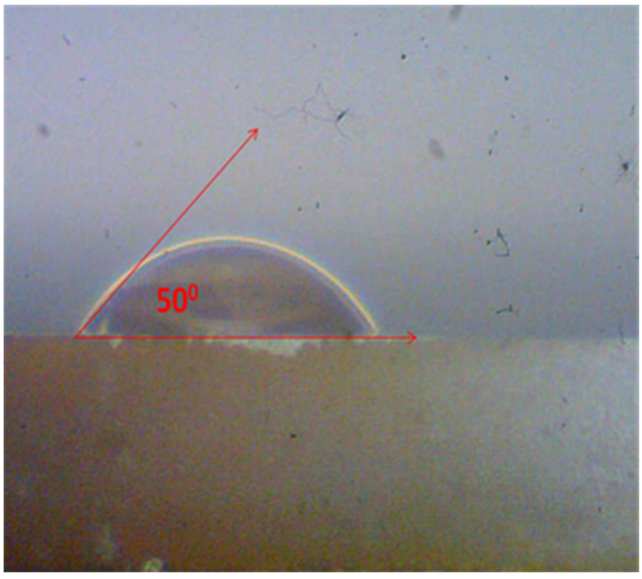

Figure 2. Schematic presentation of contact angle measurement for Sb_2S_3 films.

3.4 *Optical analysis of Sb_2S_3, SnO_2 and SnO_2/Sb_2S_3 thin films*

The wavelength dependence of optical absorption spectra of as-prepared Sb_2S_3 nanospheres was analysed in the wavelength range of 300–850 nm and the band gap was calculated. Figure 4a shows the plot of $(\text{absorbance})^2$ *vs.* $h\upsilon$ for Sb_2S_3 nanospheres. By extrapolating the lines obtained to $(\text{absorbance})^2 = 0$ on energy axis direct band gap of Sb_2S_3 was observed as 2.17 eV for the deposited Sb_2S_3 film. Such a value agrees well with the value 2.26 eV for crystalline Sb_2S_3 reported in Rajpure *et al*,[16] but it is somewhat higher than band gap energy of 1.62 eV reported by Desai and Lokhande.[17]

Figure 4b shows wavelength-dependent absorption spectra for Sb_2S_3, SnO_2 and SnO_2/Sb_2S_3. The SnO_2 film exhibits absorption around wavelength less than 340 nm, quite suitable as window material, seldom studied for semiconductor sensitized-based solar cell,[27] as compared with TiO_2.[20–22] Sb_2S_3 shows prominent peak of absorption at wavelength about 350 nm and has very promising absorbance extended into far visible region of electromagnetic waves. This makes it very appropriate absorber material for photovoltaic cells.[28]

Optical absorption spectra shown in figure 4b suggest that deposition of a Sb_2S_3 helps to enhance the photoresponse

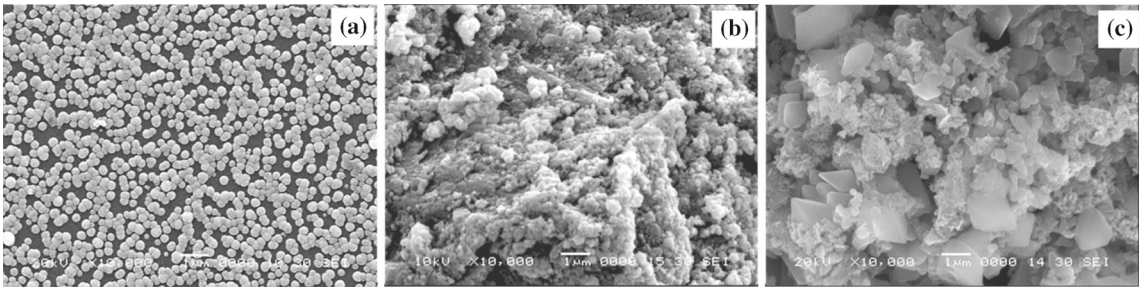

Figure 3. (**a**) Band gap calculation and (**b**) optical absorption spectra of SnO_2, SnO_2/Sb_2S_3 and Sb_2S_3.

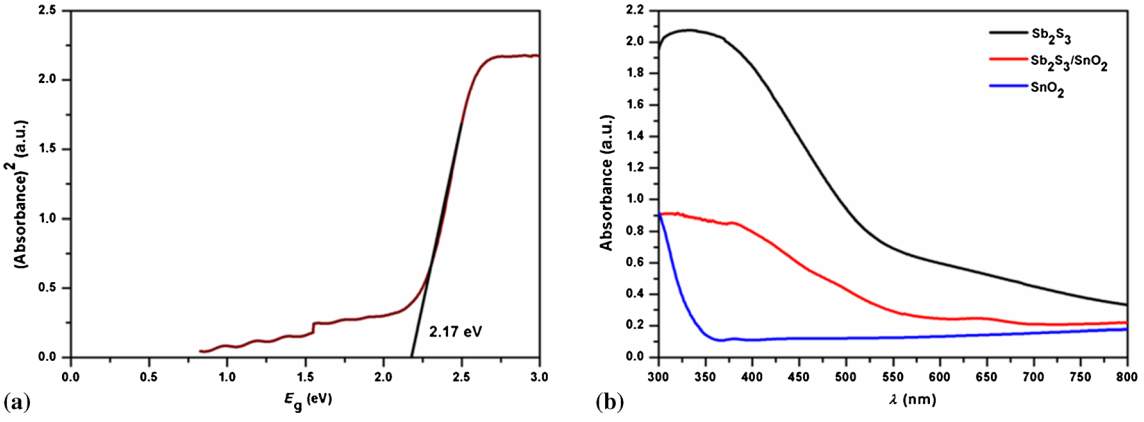

Figure 4. SEM images of (**a**) Sb_2S_3, (**b**) SnO_2 and (**c**) SnO_2/Sb_2S_3.

of the SnO_2 film by extending absorption up to 613 nm for SnO_2/Sb_2S_3 system. The enhancement in the absorbance of the SnO_2/Sb_2S_3 system in the visible region from UV-region confirms the growth of the Sb_2S_3 on the SnO_2 particles.

3.5 *Photoluminescence (PL) study of Sb_2S_3*

Figure 5 shows emission spectra for chemically deposited Sb_2S_3 measured at room temperature with excitation wavelength at 350 nm gives four distinct peaks around 472, 532, 610 and 716 nm. The first peak centred around 472, this blue emission can be attributed to deep trap states or defects in material resulted during experimental conditions.[29] Second peak about of 532 nm, corresponds to the green emission, which is in agreement with the previous study by Kulyk *et al*.[30] Third peak at 610 nm is the PL peak for deposited Sb_2S_3 and agrees well with the observations made by Xu *et al*[31] for Sb_2S_3. Fourth emission peak observed approximately at 717 nm, which is at higher wavelength than that of absorption peak approximately at wavelength of 430 nm. This observed red shift in position of emission peak can be attributed to Stoke's shift, which may be due to the localized centres in band structure.[32]

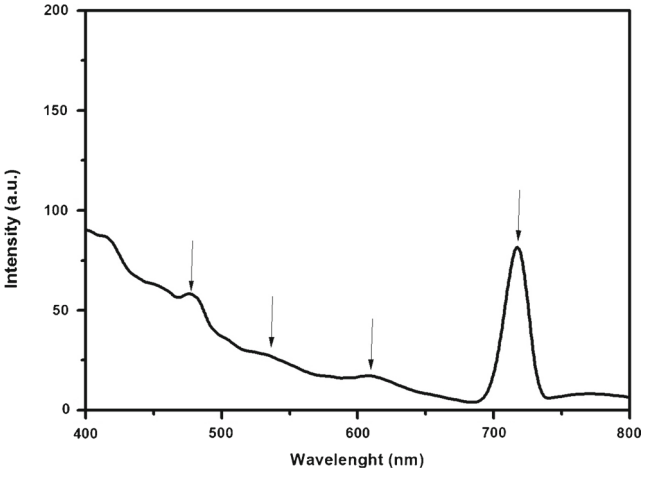

Figure 5. Room temperature PL spectrum of Sb_2S_3.

3.6 *Photovoltaic analysis*

Figure 6a presents the schematic of charge generation-transfer process for Sb_2S_3-sensitized SnO_2 photoelectrode-based solar cell. Illumination of the conducting electrode causes excitation of Sb_2S_3, excited electron will enter in the conduction band (E_c) of Sb_2S_3 and hole will remain in the valence band (E_v). The possible charge generation-transfer processes on the basis of band positions of SnO_2, Sb_2S_3 and electrolyte has been shown in figure 6b. From the energy level alignment of SnO_2 and Sb_2S_3, it is observed that the E_c of Sb_2S_3 is negative enough to inject electron into SnO_2, a wide band semiconductor, which has the conduction band edge minimum more positive as compare to TiO_2 (at −4.5 eV for SnO_2; −4.2 eV for TiO_2).[33,34] Hence the excited Sb_2S_3 can easily inject electrons from its E_c quickly into the E_c of SnO_2, as compare to TiO_2. The flakes like morphology of SnO_2 helps the received electrons to percolate through SnO_2 to the conducting FTO. Finally, it travels through the external load and complete the circuit by entering the system *via* counter electrode. The function of redox species is to quickly reduce back the excited Sb_2S_3 to its ground state and to set the system for next excitation. Thereafter, the redox species takes electrons from counter electrode for further action and the electron cycle repeats.

3.7 *Cell performance analysis*

Figure 7 represents J–V characteristics for solar cell fabricated using Sb_2S_3-sensitized SnO_2 photoelectrode having effective area of 0.25 cm^2 in the dark and under an illumination of 50 mW cm^{-2} showed $V_{oc} \sim 240$ mV and $J_{sc} \sim 0.640$ mA cm^{-2} and FF ∼35%.

Study of J–V characteristics reveals that, Sb_2S_3 a good absorber due to its optimum energy band gap, helps photoelectrochemical active SnO_2 so that it can accept electrons

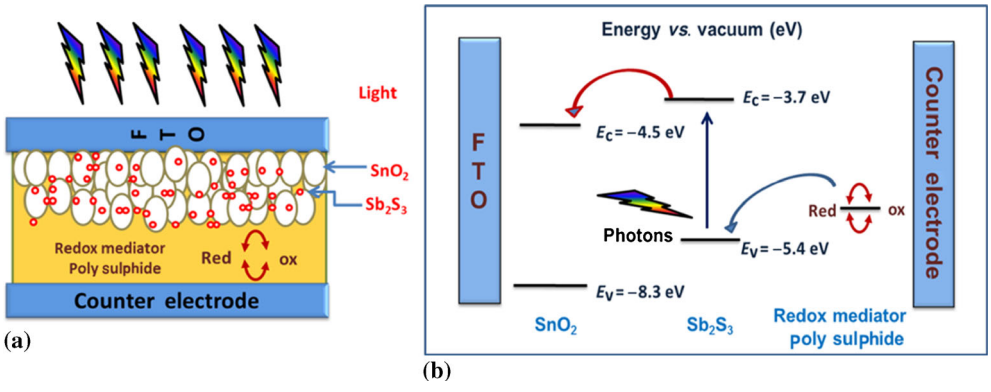

Figure 6. (**a**) Schematic presentation of nanostructured solar cell fabricated with SnO_2/Sb_2S_3 photoanode and (**b**) energy band diagram and schematic representation of charge generation and transfer process in Sb_2S_3-sensitized SnO_2-based solar cell.

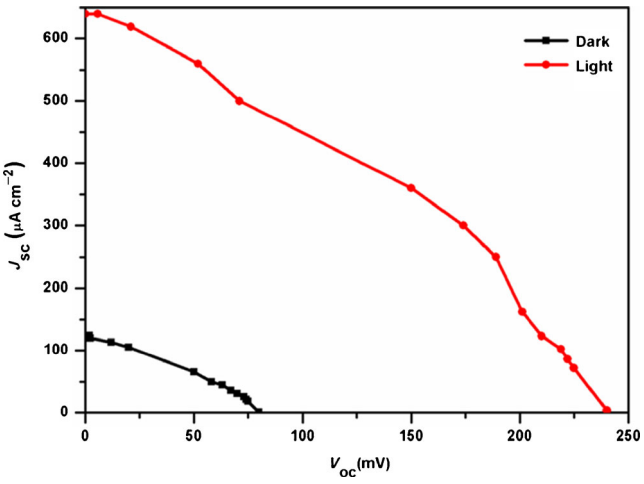

Figure 7. Photocurrent density–voltage (J–V) characteristics of Sb_2S_3/SnO_2 photoanode-based nanostructure solar cell.

from the adjacent semiconductor layer of Sb_2S_3 nanoparticles followed by efficient charge separation. This helps in the enhancement of photocurrent density by 20% for SnO_2/Sb_2S_3 system in comparison with SnO_2/CdSe system which shows $J_{sc} \sim 25$–30 μA cm^{-2} as reported by Nasr *et al*.[28] The low value of fill factor (FF $\sim$ 35%) attributes to the poor electron transfer at electrolyte–counter electrode interface. In order to improve FF it is essential to optimize electrolyte and counter electrode system for SnO_2/Sb_2S_3 photoanode-based solar cells.

4. Conclusion

In this paper, it has been reported that a template free, simple chemical route for the preparation of crystalline Sb_2S_3 nanospheres at room temperature can be a substitute for controlled and high temperature synthesis techniques. Prepared Sb_2S_3 has orthorhombic phase. Optical absorbance observed in the visible far IR-region, makes it suitable as absorber material in solar cell applications. Noticeable enhancement in absorption of visible light was observed after deposition of Sb_2S_3 over SnO_2, confirming the deposition of Sb_2S_3 onto SnO_2. The charge generation and transfer processes discussed in detail for SnO_2/Sb_2S_3-based solar cell suggest SnO_2 as an alternative to TiO_2 as well as ZnO. The photovoltaic performance for solar cell comprising SnO_2/Sb_2S_3 nanostructure shows $V_{oc} \sim 240$ mV and $J_{sc} \sim 0.640$ mA cm^{-2} and FF $\sim$ 35%.

Acknowledgements

HMP is thankful to Science and Engineering Research Board, Department of Science and Technology, New Delhi (Fast track Scheme for Young Scientists) and Departmental Research Development Program, Savitribai Phule Pune University, for financial support. SAA is also thankful to University Grant Commission, New Delhi for Faculty Improvement Program fellowship.

References

1. Rokesh K, Pandikumar A and Jothi Venkatachalam K 2013 *Mater. Sci. Forum* **771** 1
2. Jinchu I, Sreekala C and Sreelatha K 2013 *Mater. Sci. Forum* **771** 39
3. Nozik A 2008 *J. Chem. Phys. Lett.* **457** 3
4. Sun W, Yu Y, Pan H, Gao X F, Chen Q and Peng L M 2008 *J. Am. Chem. Soc.* **130** 1124
5. Zhu G, Su F F, Lv T, Pan L K and Sun Z 2010 *Nanoscale Res. Lett.* **5** 1749
6. Wang C B, Jiang Z F, Wei L, Chen Y X, Jiao J, Eastman M and Liu H 2012 *Nano Energy* **1** 440
7. Zhang Q X, Guo X Z, Huang X M, Huang S Q, Li D M, Luo Y H, Shen Q, Toyoda T and Meng Q B 2011 *Phys. Chem. Chem. Phys.* **13** 4659
8. Luan C Y, Aleksandar V, Andrei S S, Xu X Q, Wang H E, Chen X, Xu J, Zhang W J, Lee C S, Andrey L R and Juan A Z 2011 *Nanoscale Res. Lett.* **6** 340
9. Chen Y X, Wei L, Zhang G H and Jiao J 2012 *Nanoscale Res. Lett.* **7** 516
10. Chen J, Lei W and Deng W Q 2011 *Nanoscale* **3** 674
11. Chen C, Xie Y, Ali G, Yoo S H and Cho S O 2011 *Nanoscale Res. Lett.* **6** 462
12. Kieven D, Dittrich T, Belaidi A, Tornow J, Schwarzburg K, Allsop N and Lux-Steiner M 2008 *Appl. Phys. Lett.* **92** 153107
13. Wang L D, Zhao D X, Su Z S and Shen D Z 2012 *Nanoscale Res. Lett.* **7** 106
14. Maiti N, Im S H, Lim C S and Seok S I 2012 *Dalton Trans.* **41** 11569
15. Li Y, Wei L, Zhang R, Chen Y, Mei L and Jiao J 2013 *Nanoscale Res. Lett.* **8** 89
16. Rajpure K Y and Bhosale C H 2000 *J. Phys. Chem. Solids* **61** 561
17. Desai J D and Lokhande C D 1994 *Thin Solid Films* **237** 29
18. Pawar S H, Tamhankar S P, Bhosale P N and Upllane M D 1983 *Ind. J. Pure Appl. Phys.* **21** 665
19. Lokhande C D, Sankpal B R, Mane R S, Pathan H M, Muller M, Giersig M and Ganesan V 2002 *Appl. Surf. Sci.* **193** 1
20. Yafit I, Olivia N, Miles P and Gary H 2009 *J. Phys. Chem. C* **113** 4254
21. Moon S J, Itzhaik Y, Yum J H, Zakeeruddin S M, Hodes G and Gratzel M 2010 *J. Phys. Chem. Lett.* **1** 1524
22. Im S H, Kim H J, Rhee J H, Lim C S and Seok S I 2011 *Energy Environ. Sci.* **4** 2799
23. Arote S A, Ingale R V, Tabhane V and Pathan H M 2014 *J. Renew. Sustain. Energy* **6** 013132
24. Meherzi H M, Nasr T B, Kamoun N and Dachraoui M 2010 *Physica B* **405** 3101
25. Azaroff L V 1968 *Elements of X-ray crystallography* (New York: McGraw-Hill) p. 552

26. Han Q, Lu J, Yang X, Lu L and Wang X 2008 *Cryt. Growth Des.* **8** 395
27. Messina S, Nair M T S and Nair P K 2008 *J. Phys. D: Appl. Phys.* **41** 095112
28. Nasr C, Kamat P and Hotchandani S 1996 *J. Electroanal. Chem.* **420** 201
29. Alemi A, Hanifehpour Y and Joo S W 2011 *J. Nanomater.* **2011** 414798
30. Kulyk B, Kapustianyk V, Krupka O and Sahraoui B 2011 *J. Phys.: Conf. Ser.* **289** 012003
31. Xu Y, Ren Z, Cao G, Ren W, Deng K and Zhong Y 2009 *Cryst. Res. Technol.* **44** 851
32. Fujita T, Kurita K, Takiyama K and Oda T 1988 *J. Lumin.* **39** 175
33. Rhee J H, Chung C and Diau E W-G 2013 *NPG Asia Mater.* **5** e68
34. Patrick C E and Giustino F 2011 *Adv. Funct. Mater.* **21** 4663